Research, Society and Development, v. 9, n. 8, e448985463, 2020
(CC BY 4.0) | ISSN 2525-3409 | DOI: http://dx.doi.org/10.33448/rsd-v9i8.5463

Simulação computacional do fluxo de partículas de soja em uma tremonha usando fluidodinâmica computacional (*CFD*) e o método dos elementos discretos (*DEM*)

Computational simulation of soybean particles flow in a hopper using computational fluid dynamics (CFD) and discrete elements method (DEM)

Simulación computacional del flujo de partículas de soja en una tolva usando fluido dinámico computacional (*CFD*) y el método de elemento discreto (*DEM*)

Recebido: 09/06/2020 | Revisado: 26/06/2020 | Aceito: 30/06/2020 | Publicado: 13/07/2020

Jéssica Aparecida Apolinário de Paula
ORCID: https://orcid.org/0000-0002-0994-2411
Universidade Federal do Triângulo Mineiro, Brasil
E-mail: jessyap_92@hotmail.com
Érica Victor de Faria
ORCID: https://orcid.org/0000-0001-9890-7273
Universidade Federal do Triângulo Mineiro, Brasil
E-mail: erica-victor@hotmail.com
Ana Christina Pitard Lima
ORCID: https://orcid.org/0000-0002-8386-6816
Universidade Federal do Triângulo Mineiro, Brasil
E-mail: tinapitard@hotmail.com
José Luiz Vieira Neto
ORCID: https://orcid.org/ 0000-0003-0736-3974
Universidade Federal do Triângulo Mineiro, Brasil
E-mail: jose.neto@uftm.edu.br
Kássia Graciele dos Santos
ORCID: https://orcid.org/0000-0001-7452-6900
Universidade Federal do Triângulo Mineiro, Brasil
E-mail: kassia.santos@uftm.edu.br

Resumo

As tremonhas são as estruturas mais comuns usadas em unidades de armazenamento de produtos agrícolas, como grãos e cereais. A soja, que é um dos produtos mais comuns no

Brasil, passa a maior parte do tempo em uma tremonha entre as etapas de colheita e embarque. Problemas como danos às estruturas da tremonha durante a saída são fatores que foram objeto de estudos usando modelos computacionais. A Fluidodinâmica Computacional (CFD) tem desempenhado um grande papel no estudo de sistemas gás-sólido, juntamente com o Método de Elementos Discretos (DEM). Esse método gerencia a fase fluida e a fase sólida, que neste caso é granular, por meio das abordagens Euleriana e Lagrangiana. O DEM é baseado na interação entre as partículas e cada uma é monitorada separadamente. Este trabalho tem por objetivo calibrar os parâmetros do modelo mola-amortecedor, presente no estudo da dinâmica granular dos fluidos, que influencia o contato entre as partículas de soja no silo. Para este fim foi feita a comparação do tempo experimental de descarga da soja em uma tremonha, com o tempo resultante de 27 simulações geradas por um planejamento composto central (PCC). Através da análise das simulações e estatísticas, foi possível identificar os fatores que influenciam o tempo de descarga ou não e estabelecer uma calibração desses parâmetros que melhor descrevem os resultados experimentais.
Palavras-chave: Simulação computacional; Soja; Tremonha; Tempo de descarga.

Abstract

The hoppers are the most common structures used in storage units for agricultural products such as grains and cereals. The soybean, which is one of the most common products in Brazil spend most of their time in a hopper between the stages of picking and shipment. Problems such as damage to the hopper structures during the outflow are factors that have been the subject of studies using computational models. Computational Fluid Dynamics (CFD) has played a big role in gas-solid systems study, together with the Discrete Element Method (DEM). This method manages both fluid phase as the solid phase, which in this case is granular, through the Eulerian and Lagrangian approach. The DEM is based on the interaction between the particles and each one is separately monitored. This work aims to calibrate the parameters of the spring-dashpot model, in the granular dynamics of fluids study, which influences the contact between the soy particles in the silo. For this purpose, a comparison was made of the experimental discharge time of soybeans into a hopper, with the time resulting from 27 simulations generated by a central composite design (CCD). Through the analysis of the simulations and statistics, it was possible to identify the factors that influence whether or not the time of discharge and establish a calibration of these parameters that best describe the experimental results.
Keywords: Computational simulation; Soybean; Hopper; Discharge time.

Resumen

Las tolvas son las estructuras más comunes utilizadas en las unidades de almacenamiento de productos agrícolas, como granos y cereales. La soja, que es uno de los productos más comunes en Brasil, pasa la mayor parte del tiempo en una tolva entre las etapas de cosecha y envío. Problemas como el daño a las estructuras de la tolva durante la salida son factores que han sido objeto de estudios utilizando modelos computacionales. La Dinámica de Fluidos Computacional (CFD) ha jugado un gran papel en el estudio de los sistemas de gas sólido, junto con el Método de Elementos Discretos (DEM). Este método gestiona la fase fluida y la fase sólida, que en este caso es granular, utilizando los enfoques Euleriano y Lagrangiano. El DEM se basa en la interacción entre las partículas y cada una se controla por separado. Este trabajo tiene como objetivo calibrar los parámetros del modelo "muelle-amortiguador", en el estudio de dinámica granular de los fluidos, que influyen en el contacto entre las partículas de soja en el silo. Para este propósito, se hizo una comparación del tiempo experimental para descargar la soja en una tolva, con el tiempo resultante de 27 simulaciones generadas por una planificación compuesta central (PCC). Mediante el análisis de las simulaciones y estadísticas, fue posible identificar los factores que influyen o no en el tiempo de descarga y establecer una calibración de estos parámetros que mejor describan los resultados experimentales.

Palabras clave: Simulación computacional; Soja; Tolva; Tiempo de descarga.

1. Introduction

Silos are extremely important in several industries, mainly agriculture with advantages of efficient use space, stock storage, the supply of the manufacturing process, such as grains and cereals. One of the most important steps in the agricultural processing of grain is the storage because they are stored until they are dispatched. So the grains must be stored in locations that provide the necessary conditions so that it does not suffer any deterioration (Batista, 2009). However, these structures are complex to design, with various geometry formats, and often presenting operational problems due to the kind of flow inside them, since there are different types of products that can be stored.

The use of simulations has been gaining strength to represent granular multiphase systems, such as silos and hoppers, due to the possibility of obtaining the flow patterns inside these devices, which in most cases is difficult to visualize during their operation. In the case of multiphase systems, there are 2 main approaches that can be used: Computational Fluid

(CC BY 4.0) | ISSN 2525-3409 | DOI: http://dx.doi.org/10.33448/rsd-v9i8.5463

Dynamics (CFD) simulations by finite volume technique using an Eulerian approach or the Discrete Element Method (DEM) using a Lagrangian approach. And there is also the possibility of applying the 2 together in CFD-DEM simulations with a Euler-Lagrange approach, which is what will be used in this work, treating the fluid flow via CFD and the granular particles by DEM. These numerical methodologies as well as works in the literature that employ them will be detailed in the topics following this paper.

This work has as objective the calibration of Spring-dashpot model parameters, in granular fluid dynamics, influencing the contact between the particles of soybeans in the silo. The parameters will be simulated by a CFD-DEM approach in different combinations according to the central composite design (CCD) and subsequently, their results are compared with the experimental discharge time and so will be better defined set of parameters.

2. Silos Geometry

The type of the silo used must be decided according to the material necessities for the storage. Having that in mind, some characteristics inside the silo must be analyzed, for example, the geometry of the silo, its material properties as well as the solid material. The silos may be classified according to its geometry, the type of discharge flux, the orifice discharge configuration among others. The surface level is one of the parameters, being raised silo or lower silo the types used. According to the relation between the height and diameter, it can be horizontals, shorts, or slims; also the air inlet may be not hermetic or hermetic (Vieira, 2009). The bottom of the silo is called hopper which has the function to facilitate the flow of the particles contained inside the silo and also influences the flow because of its geometry (Vieira, 2009). The hopper's classification of geometry is shown in Figure 1 (Cheung, 2007).

Figure 1 – Geometry hopper’s type.

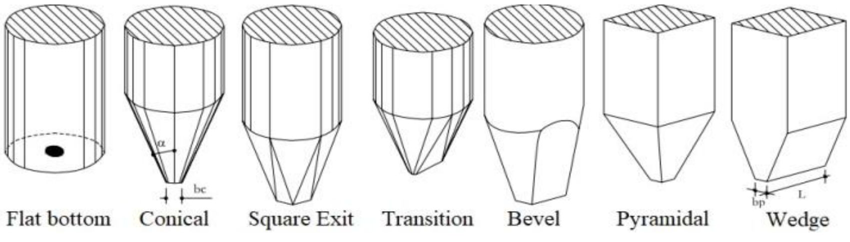

Source: Adapted from Cheung (2007).

There are several hopper geometries for storage systems as can be seen in Figure 3. They are divided into two main types of hoppers, flat flow, and axisymmetric flow. Flat flow is when the product has its flow characterized by a plane. Axisymmetric flow is when the product has its flow in the 3 main directions. According to Jenike (1964), wedge hoppers (flat flow) allow for slightly higher inclinations (usually from 8 to 10°) for products with the same physical properties, as they present higher stable arc tensions in imminent flow. Therefore, the wedge hopper requires lower height when compared to the conical hopper (axisymmetric). Therefore, the size of the outlet mouth b_c for the axisymmetric hopper is usually greater than the width b_p for the wedge hopper. The disadvantage of the wedge hopper is that the opening is $L = 3.b_p$, which in practice, is much smaller than the width of the silo. For this reason, the hopper in transition has been used more (Cheung, 2007).

According to Palma (2005), in the case of silos with funnel flow, the angle of inclination of the hopper with the vertical is greater than for the mass flow. Therefore, the hopper, for this type of flow, has a lower height and can be used in places where the height of the silo is limited. However, depending on the product to be stored, they may need flow-promoting devices such as bin inserts to restore flow when, for example, a tube-shaped obstruction is formed.

3. The Flow

Medeiros (2012) describes the solids flow as a movement that is caused by particle-particle contact and between the particles and the silo walls. The solid flux inside of the silo is different from the liquid flux, and cannot be established the same properties for them.

According to Calil Junior & Cheung (2007) the flow of a solid is influenced by the geometric characteristics of the silo and the characterization of discharge contained within, as well as the type of segregation, as well as check if there are stagnation zones.

During the runoff, some flow zones are formed inside the silo. These vary according to the change of position of the product that is being unloaded. According to Brown & Nielsen (1998), there are five regions, or areas that characterize the flow. These regions are described in Figure 2.

Figure 2 – The flux zones.

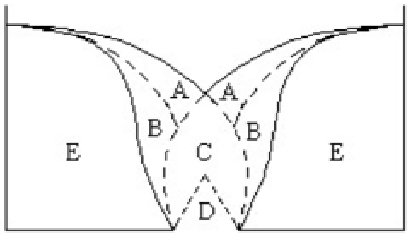

Source: Brown & Nielsen (1998).

Figure 2 shows zone A, the area where the particles flow spontaneously and will losing speed, forming zone B. When the particles arrive in zone C they accelerate and go for zone D where they lose contact with the neighborhood and are unloaded. The zone E, is a stagnation area, in this zone has almost no change of movement during the runoff.

Jenike (1964) classified into two types of flux, the mass flow, and the funnel flow. Figure 3 shows an illustrative scheme that differentiates these flow types (DIN 1055, 1987 *apud* Batista, 2009).

Figure 3 – Flow types in hoppers.

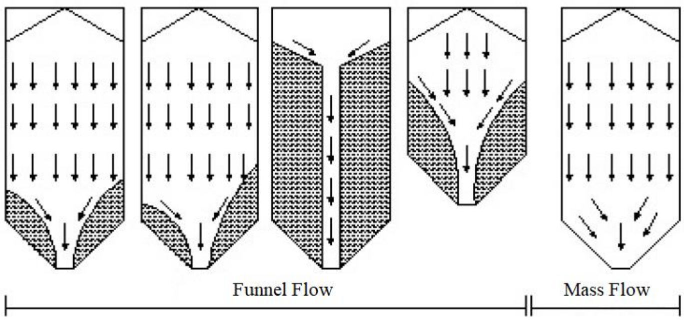

Source: Adapted from Batista (2009).

Describing the types of flow in Figure 3, it can be noted that the movement of the particles in all parts of the silo at the time of unloading characterizes the mass flow, this occurs when the hoppers used are smooth, steep, and abrupt transitions-free. The funnel flow is characterized by the movement of only a few particles, i.e. formed a preferred path in the center of the silo where they will descend and stagnation zones on the sides. This phenomenon occurs when the walls of the hopper are roughened and the tilt angle with the vertical is great (Batista, 2009).

In Table 1, Calil Junior & Cheung (2007) and Vieira (2009) established the characterization of the main advantages and disadvantages of mass flow and funnel.

Table 1 – Advantages and disadvantages of mass and funnel flow.

Mass Flow		Funnel Flow	
Advantages	**Disadvantages**	**Advantages**	**Disadvantages**
Regular flow	High tension in the transition from the hopper	Lower hopper height	Fluctuations in flow rate
The radial segregation effect is reduced with improved homogeneity	Wall surface wear	Reduction of dynamic pressure in the hopper	Consolidation effects over time may cause obstructions in stream
More predictable stress field	There is a need for deeper hoppers	Minor surface wear from the wall	The collapse is favored
The whole capacity is used	Greater lifting power	-	Reduction of storage capacity
Greater storage capacity, does not have areas with stagnant product	The particles must resist the fall of greater heights	-	Forming paths

Source: Adapted from Calil Junior & Cheung (2007) and Vieira (2009).

Knowing the characteristics of each flow, you can choose the best-operating conditions. The silos should be designed to have conditions to store and unload the product of interest in the best possible way, that is, with the lowest numbers of errors because such errors can generate negative effects both in equipment and product structure (Batista, 2009).

In addition, the flux is also influenced by the properties of the particles, as the contact forces between the particles with each other, the particles with the wall, and the gravitational force (Medeiros, 2012). For example, the solid flow decreases with the increase in the moisture content of the particles and this acquires viscous properties that harm the shear tests, used to identify the product and flow properties.

4. The Numerical Model

With the accessibility of computers and the development of software using these programs is increasingly present in engineering projects and has become a valuable tool for research. The mathematical models along with the numerical methods are used for the solution of complex problems and implemented in computer programs. The use of computer programs has the advantage of speed in getting results, ease access to ready programs and a range of properties that can characterize the object of study (Justin, 2012).

As is the case of simulations by CFD (Computational Fluid Dynamics) which has been used as a numerical tool powerful that assists in obtaining information of multiphase systems, solid-gas, heat transfer, in addition to cover industrial and non-industrial areas leading to cost reductions and project time (Justin, 2012).

CFD simulations have gained prominence in studies of heat, mass, and momentum transfers phenomena in various devices, such as spouted beds (Vieira Neto et al., 2008; Cunha et al., 2009; Bortolotti et al., 2013; Santos et al., 2015; Santos et al., 2017; Batista Junior et al., 2019); fluidized beds (Müller et al., 2009; Araújo & Santos, 2017); fixed beds (Béttega et al., 2013, Rocha et al., 2020; Stoppe et al. 2020); rotational disk granulators (Vieira Neto et al., 2017); dryer drums (Silvério et al., 2014; Cunha et al., 2016; Gravena et al., 2019); solar dryers (Krawczyk & Badyda, 2011; Tegenaw et al., 2019; Rocha et al., 2020; Stoppe et al. 2020); concentric and eccentric annuli (Neto et al., 2011; Vieira Neto et al., 2014); horizontal injector wells (Mantegazini & Romero, 2019) and waste treatment tank (Pereira & Góis, 2020).

The use of this technique involves the treatment of two phases in question through the Eulerian approach-Eulerian, applied to the fluid, and the Eulerian-Lagrangian approach, applied to the solid phase (Marques, 2013).

The Eulerian model Granular use when the volume fraction of the granular phases and still are comparable or so when the gravitational force or the interaction between phases influence the fluid dynamics of the system. Kinds of phases are important in the characterization of the system, because for each stage is solved a set of equations of moment and of continuity, as well as influence on the type of pressure coupling (Araújo, 2014).

5. Discrete Element Method (DEM)

Computational Fluid Dynamics - CFD has been a valuable tool in the study of granular systems. With an Eulerian-Eulerian and Eulerian-Lagrangian approach. It is possible to study the fluid and granular phases and characterization of parameters for both of them (Marques, 2013).

The grains have a certain difficulty being studied since the nature of the medium is mild and they interact individually. They particles can collide with the neighboring particles or the wall and this contact can be described by DEM. The Discret Element Model is a model used in multiphase systems where it treats the particles as independent sets and interact with each other explaining the discrete nature of granular media (Neves, 2009 *apud* Lima, 2014).

The analysis of silos using the DEM has been fairly applied. Höhner et al., 2015, conducted a study on the influence of geometric shape of granular particles in the mechanical interactions using the DEM method the results identified the reduction of particle sphericity changed the characteristics of the stream. Balevičius et al. (2011) used the DEM method to compare the particle flow behavior in different geometries of silo, the results identified that the output speed and the total discharge time is affected by the geometry of the silo. Montellano et al. (2011) *apud* Lima (2014) developed a three-dimensional model to simulate flow of corn, the results identified the properties of friction were not relevant in the discharge flow influence.

As for the calibration of parameters of soya beans, Almeida, 2015 conducted simulations in a rotating drum of countertop filled with soy. The discrete element method by the *software FLUENT ® 14*, various simulations were carried out with different combinations of the values of coefficients of restitution, friction and elasticity, which are parameters to the linear model "spring-damper. Through the comparison of simulations with the experimental data of the dynamic angle of repose, found that the most influential variable in this system was the friction coefficient with a value of 0.2.

6. Material and Methods

A laboratorial and quantitative research method was used in the present experimental and CFD-DEM simulation study. The methodological support for the experiments and numerical simulations were following described (Pereira, 2018).

The soybeans grains were the granular material studied, and it by its time has a ellipsoidal form, the characteristics of this particle are 6.13 mm of diameter, 1.289 g/cm³ of density and mass of 0.156 g for each particle. Figure 4 shows the silo used in the experiments.

Figure 4 – Silo used for soybean discharge time experiments.

Source: Authors (2020).

The cylindrical part contains dimensions of 0.237 m in height, 0.29 m in diameter in the cylindrical and the conical part is 0.066 m high, with an outlet diameter of 0.043 m. With these characteristics, the silo has an H/D ratio equal to 1.04 which characterizes it as an intermediate silo according to the Australian standard As3774.

The Hopper was put above a digital balance and filled with 2.3 and 4.0 Kg of soybean grains. This was repeated three times. The soy discharge was filmed, which enabled to identify the mass discharged and its time.

6.1 Achievement of discharge time through simulation

In order to evaluate the effect of some parameters of the DEM discharge time was made an experimental design using the software *STATISTIC*, which was the base of the simulations on *FLUENT ® 14.* The central composite design (CCD) proposed to evaluate the constant of elasticity (K), the coefficient of restitution (η), the coefficient of friction (μ_f), and the rolling coefficient (μ_r) and had three replicas on the central point. Table 2 that follows shows the variables codifications of the CCD.

Table 2 - Coded variables of CCD.

Variables	Levels				
	-1.54671	**-1.0**	**0.0**	**1.0**	**1.54671**
X_1: K [N/m]	71.97535359	400	1000	1600	1928.25
X_2: η [–]	0.035987677	0.2	0.5	0.8	0.964012
X_3: μ_f [–]	0.040658451	0.15	0.35	0.55	0.659342
X_4: μ_r [–]	0.040658451	0.15	0.35	0.55	0.659342

Source: Authors (2020).

Table 2 shows the range of values for each of the variables studied within the 5 levels of the CCD. The values of $-\alpha$ and $+\alpha$ levels were -1.54671 and +1.54671 that represent the extremes levels in this CCD. Therefore, the constant of elasticity (K), variable X_1, had a value range between 71.97535359 and 1928.25 N/m, the coefficient of restitution (η), variable X_2, between 0.035987677 and 0.964012, and so on.

6.2. Computational simulations

The CFD simulation was made by the software *FLUENT* ® *14.0,* the mesh generated by the software *Gambit* ® 2.4.6. The hexahedral mesh mapped with 1247 cells was drawn with a bigger diameter than the soy size, in a way to allow that the particles settled and fell down.

In the software *FLUENT* ® *14.0* is possible to work with a continuous phase through the Eulerian model and also the discrete phase (soy) through the DEM that addresses the Lagrangian model, through a CFD-DEM approach.

The Eulerian model that describes the continuous phase, may be described by the equation of continuity and the movement's conservation, as follows:

$$\frac{\partial \rho}{\partial t} + \nabla\left(\rho \vec{v}\right) = 0 \qquad (1)$$

$$\frac{\partial}{\partial t}\left(\rho \vec{v}\right) + \nabla\left(\rho \vec{v}\vec{v}\right) = -\nabla \rho + \nabla\left(\bar{\bar{\tau}}\right) + \rho \vec{g} + \vec{F} \qquad (2)$$

The DEM is expressed by the contact force and the movement calculation of particles using the second Newton's Law. Firstly, the interaction forces are calculated by the interaction between the particles, on the second stage the Newton's Law is used to solve the particles movement that is made from ordinary equations. This has the forces that act in the particle or may be originated by the chock with other particles or the flow surface, gravitational forces or waves originated from particles that are not in touch with the fluid.

$$m\frac{d\vec{v}_p}{dt} = \vec{F}_{drag} + \vec{F}_{pressure} + \vec{F}_{virtual\,mass} + \vec{F}_{gravitational} + \vec{F}_{others} \qquad (3)$$

$$\vec{v}_p = \frac{dx}{dt} \qquad (4)$$

Where $\vec{v}_p$ is the particle's velocity, *x* is the position and *t* is the time.

7. Results and Discussion

The curves that relate the mass and discharge time for three different mass of the soybean are showed in Figure 5. It was noticed that these curves had the same tendency independent of the mass used.

Figure 5 – Experimental curves of mass versus discharge time.

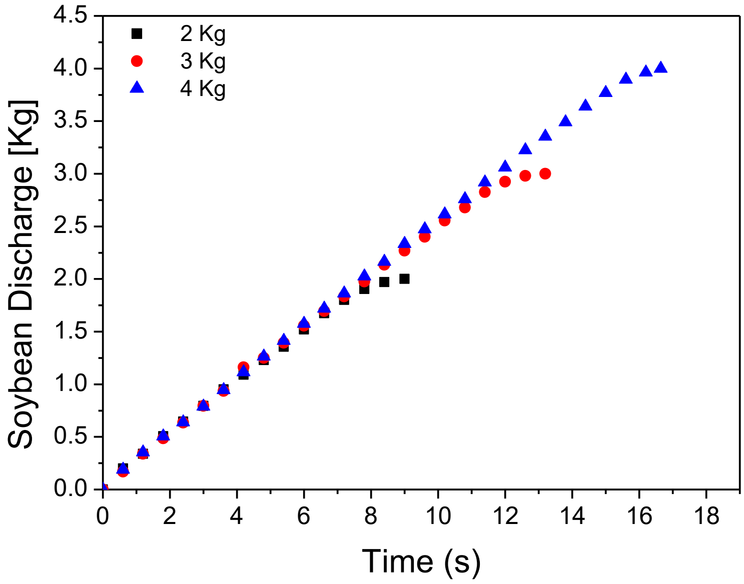

Source: Authors (2020).

The CFD-DEM simulations were conducted in accordance with each set of parameters provided by the CCP. The discharge time and masses got in the simulations are in Table 3. It was noticed that some simulations provided a discharge time similar to the experimental result while other were discrepant. In some cases the particles weren't totally discharged of the silo. The closer discharge time the experimental value was given by the simulations 2, 6, 10 and 14 where the coefficient of friction (μ_f) -1 level, whose value is 0.15, was the parameter in common between them.

Table 3 - Discharge time from Simulations.

Simulation	K	η	μ_f	μ_r	Time (s)	Mass (Kg)
1	-1.00000	-1.00000	-1.00000	-1.00000	7.20	2.00
2	-1.00000	-1.00000	-1.00000	1.00000	8.70	2.00
3	-1.00000	-1.00000	1.00000	-1.00000	42.70	1.74
4	-1.00000	-1.00000	1.00000	1.00000	85.20	1.73
5	-1.00000	1.00000	-1.00000	-1.00000	7.70	2.00
6	-1.00000	1.00000	-1.00000	1.00000	8.70	2.00
7	-1.00000	1.00000	1.00000	-1.00000	34.70	1.81
8	-1.00000	1.00000	1.00000	1.00000	58.20	1.71
9	1.00000	-1.00000	-1.00000	-1.00000	7.10	2.00
10	1.00000	-1.00000	-1.00000	1.00000	8.60	2.00
11	1.00000	-1.00000	1.00000	-1.00000	77.35	1.74
12	1.00000	-1.00000	1.00000	1.00000	83.35	1.73
13	1.00000	1.00000	-1.00000	-1.00000	7.35	2.00
14	1.00000	1.00000	-1.00000	1.00000	8.85	2.00
15	1.00000	1.00000	1.00000	-1.00000	37.60	1.91
16	1.00000	1.00000	1.00000	1.00000	48.20	1.72
17	-1.54671	0.00000	0.00000	0.00000	12.70	2.00
18	1.54671	0.00000	0.00000	0.00000	13.20	2.00
19	0.00000	-1.54671	0.00000	0.00000	14.85	2.00
20	0.00000	1.54671	0.00000	0.00000	13.20	2.00
21	0.00000	0.00000	-1.54671	0.00000	6.70	2.00
22	0.00000	0.00000	1.54671	0.00000	59.20	1.71
23	0.00000	0.00000	0.00000	-1.54671	10.70	2.00
24	0.00000	0.00000	0.00000	1.54671	16.20	2.00
25	0.00000	0.00000	0.00000	0.00000	13.20	2.00
26	0.00000	0.00000	0.00000	0.00000	13.20	2.00
27	0.00000	0.00000	0.00000	0.00000	13.20	2.00

Source: Authors (2020).

The statistical analyses were done to understand the relation of the parameters with the response. The analysis used a 0.10 of a level significance, and except of the constant of elasticity (K) all others parameters were significant.

In Table 4 there are some characteristics, only to the significant parameters, of statistical analysis. Through them it was possible to identify that the coefficient of friction (μ_f) was the most significant parameter in this simulation either in linear form as quadratic. It has a positive effect meaning that when it increases, also increases the discharge time. In the other hand the parameter (η), coefficient of restitution, has negative effects on the response. So, when it increases the discharge time decreases. The interaction between the friction and rolling coefficients (X_3X_4) has a positive effect on the response, since each one has the same behavior, their increase raises the time.

(CC BY 4.0) | ISSN 2525-3409 | DOI: http://dx.doi.org/10.33448/rsd-v9i8.5463

Table 4 - Table of Effects.

Factor	Effect	Deviation	p	Confidence limit -95%	Confidence limit 95%
Média	17.3567	2.858389	0.000006	11.3942	23.31915
η: $\mathbf{X_2}$	-10.2005	4.344177	0.029267	-19.2623	-1.13875
μ_f: $\mathbf{X_3}$	46.8109	4.219256	0.000000	38.0097	55.61214
$\mathbf{X_3^2}$	23.7723	5.669895	0.000448	11.9451	35.59951
μ_r: $\mathbf{X_4}$	9.0871	4.219256	0.043641	0.2859	17.88829
$\mathbf{X_2\ X_3}$	-14.5431	4.997301	0.008655	-24.9673	-4.11892
$\mathbf{X_3\ X_4}$	9.9089	4.813296	0.052792	-0.1314	19.94927

Source: Authors (2020).

.

The equation for this model is given by the values on the effect column followed by the coded parameters. So, the discharge time that represents this model can be expressed through equation (5) with R^2= 0.8915:

$$t = 17.3567 - 10.2005X_2 + 46.8109X_3 + 23.7723X_3^2 + 9.0871X_4 - 14.5431X_2X_3 + 9.9089X_3X_4 \quad (5)$$

The physical analyze for this response is that the contact between the particle and the wall generate friction in the same way that the particle-particle contact also generate. So this friction forces acting on the system hampers the free flow of these particles, and they take longer time to empty the silo.

The surface curves were plotted by the variables that influenced the best answers. In Figure 6, which relates the rolling (X_4) and restitution (X_2) coefficients.

(CC BY 4.0) | ISSN 2525-3409 | DOI: http://dx.doi.org/10.33448/rsd-v9i8.5463

Figure 6 - Curve surface of rolling (X_4) and restitution (X_2) coefficients.

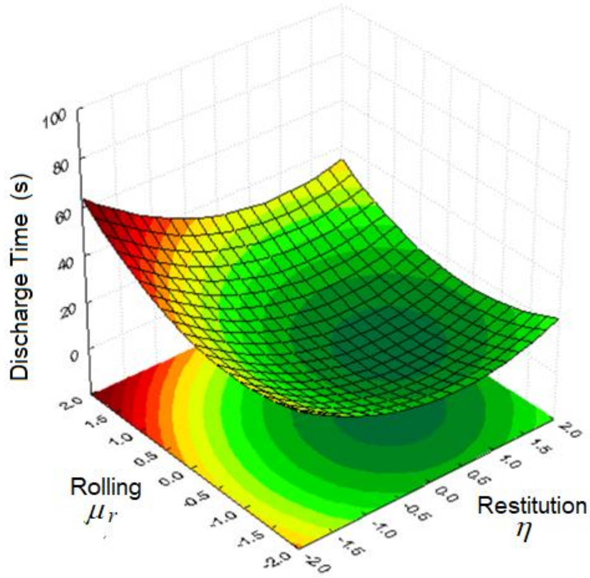

Source: Authors (2020).

Figure 6 shows that the discharge time values are larger as they increases the rolling coefficient (X_4) and when the coefficient of restitution (X_2) increases the discharge time tends to decrease. Figure 7 presents the surface response which relates friction (X_3) and restitution (X_2) coefficients.

Figure 7 - Curve surface of friction (X_3) and restitution (X_2) coefficients.

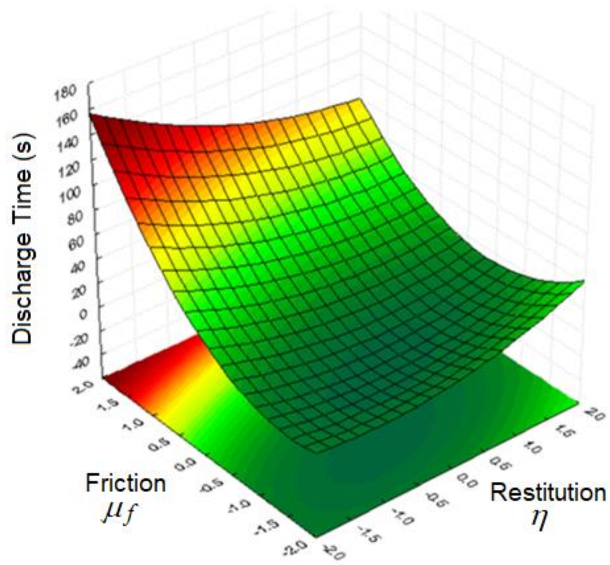

Source: Authors (2020).

(CC BY 4.0) | ISSN 2525-3409 | DOI: http://dx.doi.org/10.33448/rsd-v9i8.5463

Figure 7 displays that the discharge time values are higher as increases the friction coefficient (X_3) and decreases the restitution coefficient (X_2). These values are higher when compared with those got in Figure 6.

Through the time data of Table 3 and the statistical analysis of Table 4 was identified that the friction coefficient (X_3) was the parameter that had more influence on the simulations.

Thus, in order to assist in the selection of the set of parameters that represents the contact between the soybean particles, the simulated data of the temporal profile of the mass discharge of the solids were compared with the experimental data, as shown in Figure 8, and were grouped according to with the value of the friction and rolling parameters, since they were the most significant variables.

(CC BY 4.0) | ISSN 2525-3409 | DOI: http://dx.doi.org/10.33448/rsd-v9i8.5463

Figure 8 – Comparison of the experimental and the simulated solid discharge time profiles under the conditions: (a) μ_f =0.15 and μ_r =0.15; (b) μ_f =0.15 and μ_r =0.55; (c) μ_f =0.55 and μ_r =0.15; (d) μ_f =0.55 and μ_r =0.55; (e) μ_f =0.35 and μ_r =0.35; (f) $+\alpha$ and $-\alpha$.

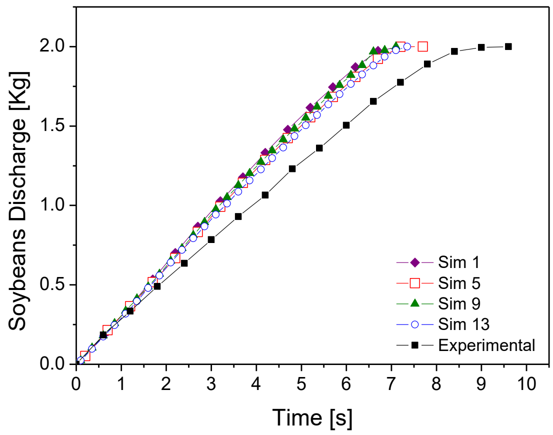

(a) μ_f =0.15 and μ_r =0.15

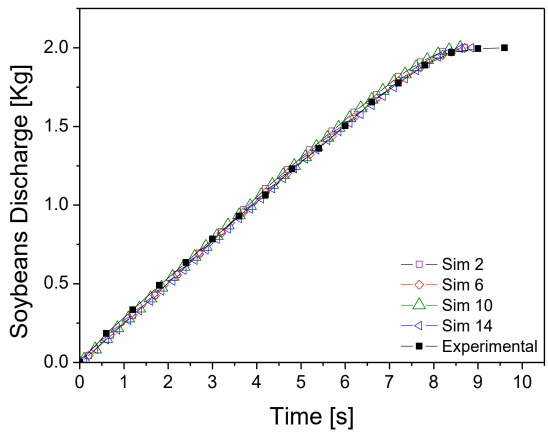

(b) μ_f =0.15 and μ_r =0.55

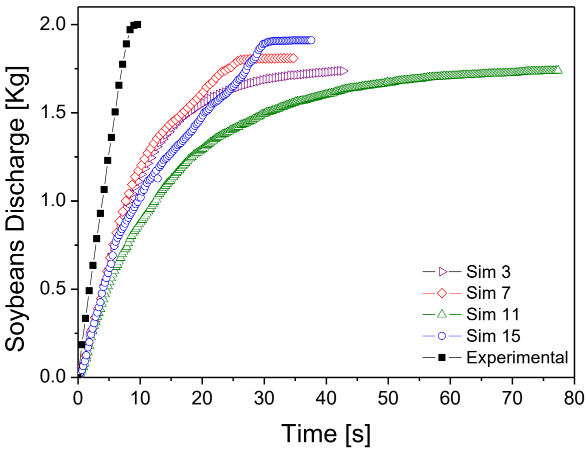

(c) μ_f =0.55 and μ_r =0.15

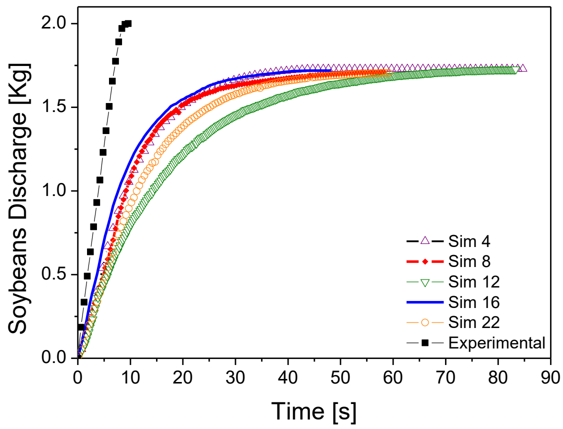

(d) μ_f =0.55 and μ_r =0.55

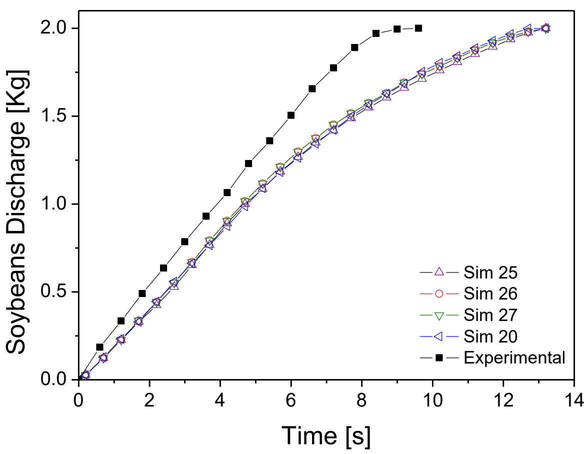

(e) μ_f =0.35 and μ_r =0.35

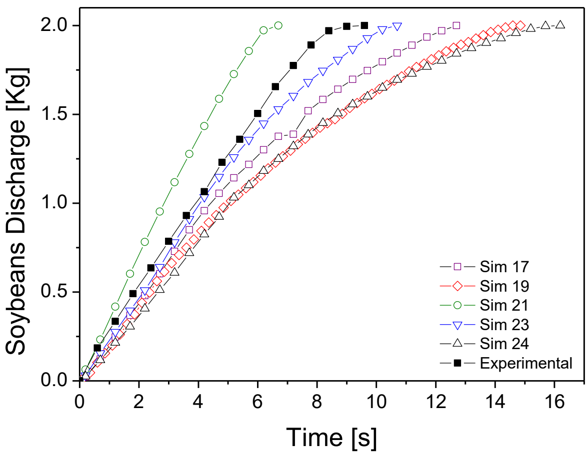

(f) $+\alpha$ and $-\alpha$.

Source: Authors (2020).

It was noticed in Figure 8b that the response that came closer to the experimental values were obtained for the simulation in which the coefficient of friction (μ_f) was 0.150 and the rolling coefficient (μ_r) was 0.550, related to the simulations 2, 6, 10 and 14 which the curves are so similar that can be confused. These show that not only the time but the mass also follows a standard and there was nothing is raising in another way. Even with such similarity the simulation that got the best time in this group was 14 but it didn't get the same value of experimental discharge time as required.

In Figure 8a, in which the friction and rolling parameters were lower, the time was slightly less than expected. As the rolling coefficient increased, this response increased and resulted in a small increase in time.

However, when the two parameters increased, the time increased considerably and part of the particles became retained in the silo (Figures 8c and 8d). This was due to the fact that the friction between particle-particle and particle-wall hinder the flow of particles because even with the gravitational force acting on them, the frictional force is greater.

Figure 8e contains the simulations of the central point and shows that they had the same curves because their results were the same, which was already expected. In this same figure, simulation 20 was added, whose only parameter with a different value was the restitution coefficient, which presented a behavior similar to that of simulations at the central point. Figure 8f shows the simulations in which one of the variables is at the +α and -α level, while the others are maintained at the intermediate level. These parameters generate differences in responses in which the discharge times were very different and all particles were discharged.

From the analysis of the solid mass discharge profiles and the statistical analysis, it was identified that the parameter that most influenced the discharge time was the static friction coefficient (μ_f) followed by the rolling coefficient (μ_r). However, there are a number of combinations between parameters that can result in the same discharge time. Silvério (2014) presented a literature review, with the range of friction coefficients used for different materials, and the friction coefficient in most works had values below 0.5, as is the case with corn, with μ_f = 0.34. Almeida et al. (2015) selected value of μ_f = 0.20 and μ_r = 0.20 for soybeans as the values that best represented the contact between the particles in a rotating drum, adequately reproducing their dynamic resting angle.

Simulations were performed with the friction coefficient μ_f being 0.15; 0.35 and 0.55. Knowing it has a positive effect on the time of discharge, it can be considered that by increasing this value from a range of 0.150 and 0.350 there is the possibility of finding a closest response to the experimental time. So, it was found in the literature a value $\mu_f = 0.20$ for the friction coefficient for the CFD-DEM simulations with soybeans. More simulations were performed using the values from 0.20 and 0.25 that generated 8.2 and 9.2s. Therefore, through these results it was possible to get close to the required experimental value.

Figure 9 presents the curves of simulation 14 the new simulation condition (A1) with $\mu_f = 0.25$ and the experimental curve.

Figure 9 - Curves comparing simulation A1, 14, and experimental data.

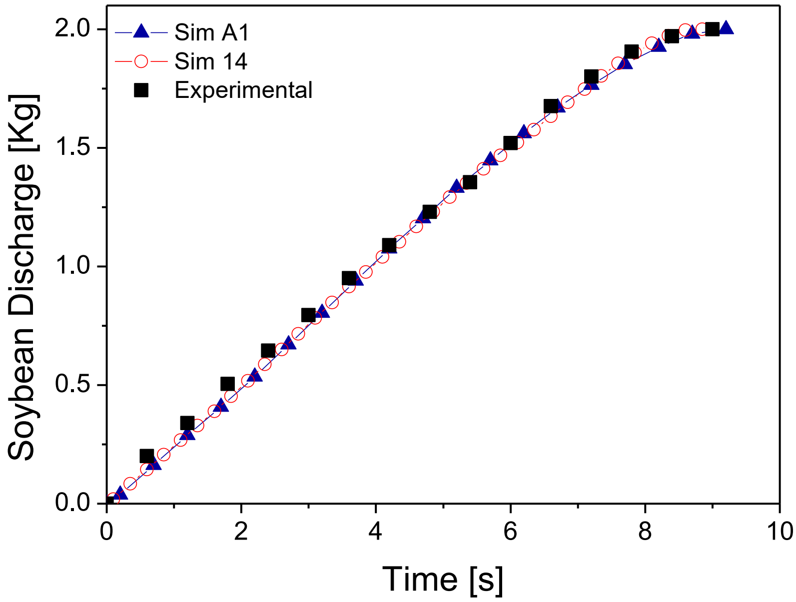

Source: Authors (2020).

It can be noted through Figure 9 the similarity between curves of simulation 14 and new simulation condition (A1), in which both had a good agreement to the experimental data.

Another representation of this similarity is in Figures 10 and 11 that show what occurs inside the silo during de discharge for these both conditions treated previously.

Figure 10 – Discharge of soybeans, colored by particle velocity (m/s) on axial z, for simulation 14 (μ_f = 0.15; μ_r = 0.55).

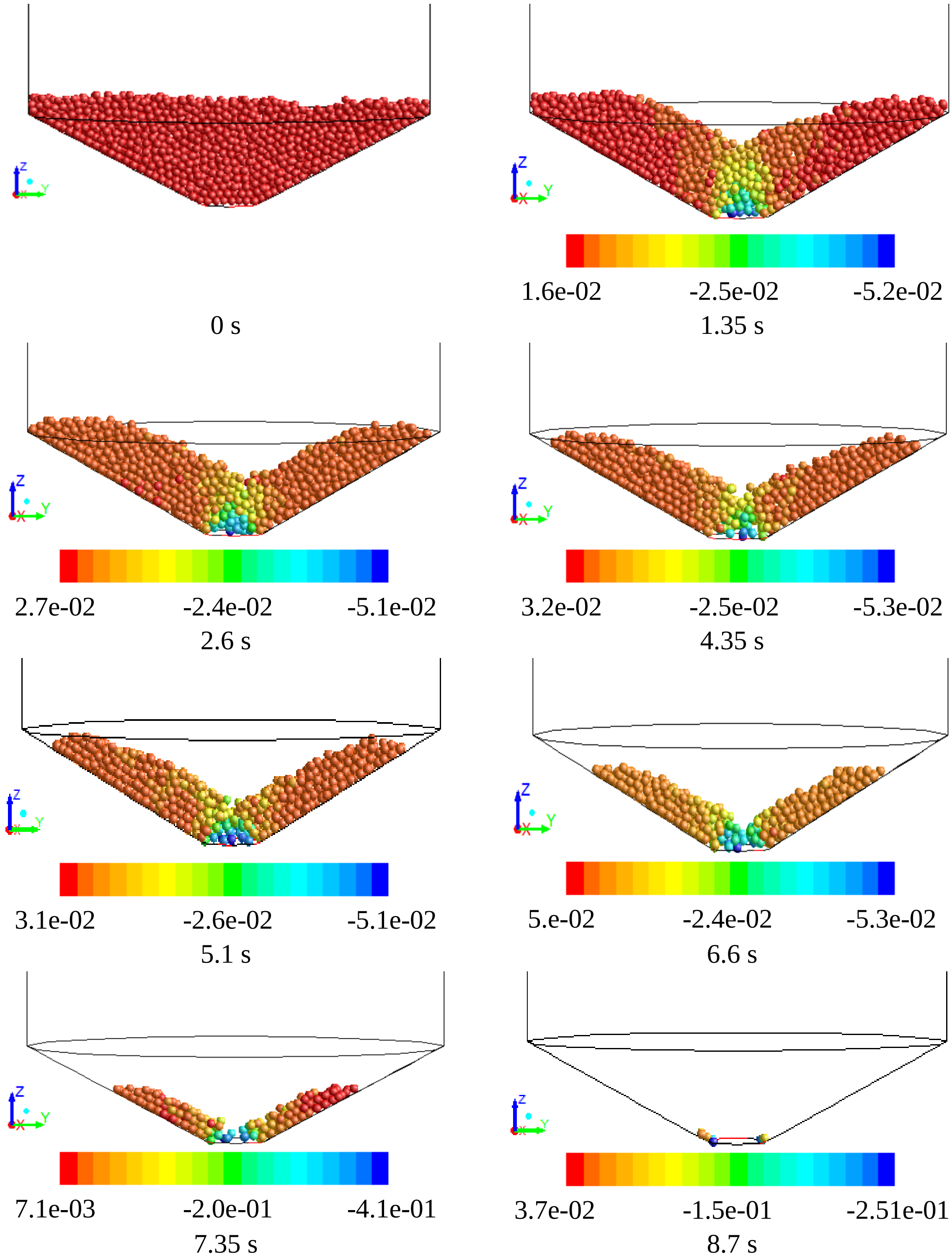

Source: Authors (2020).

Figure 10 displays that the number of particles inside the silo gradually decreases as the discharge time passes and that with 8.7 seconds it has practically emptied the hopper.

Figure 11 – Discharge of soybeans, colored by particle velocity (m/s) on axial z, for simulation A1 ($\mu_f = \mu_r = 0.25$).

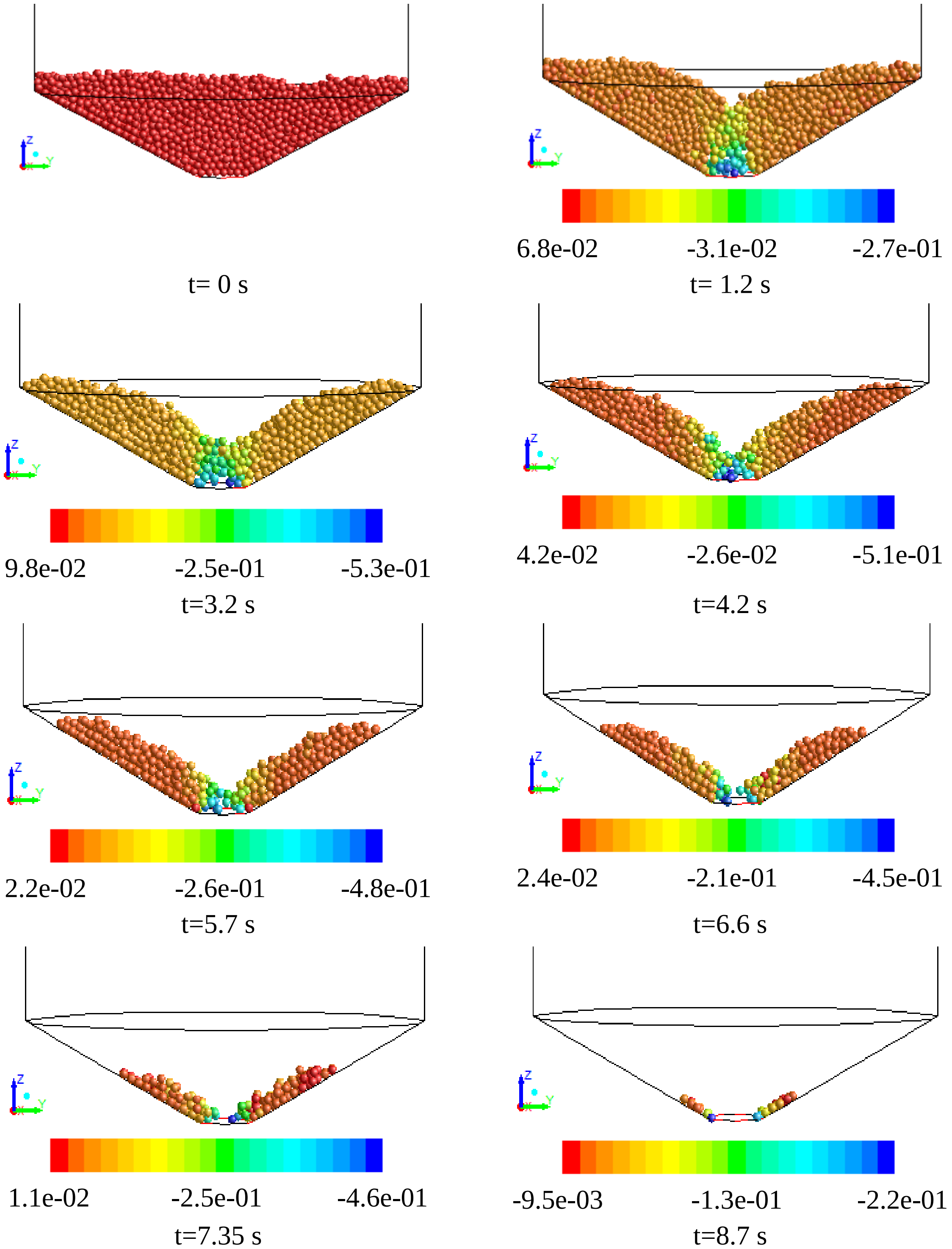

Source: Authors (2020).

Figure 11 show that the number of particles inside the silo gradually decreases as the discharge time passes and that with 8.7 seconds it has practically emptied the hopper, although with more particles than Figure 10 because the simulated time in this condition is 9.2 seconds.

As the silo was made of metal was not possible to see what type of flow occurring during the discharge. Then, a way of identifying the flow is through simulation, as Figures 10 and 11 which contains the best simulations and are colored according to the particle velocity in the z-axis. In both figures it is observed that the speed near the outlet section is larger and the lateral this speed is very low, thus creating a stagnation zone in the silo. The particles create a preferred path in the center and will leaking until you reach the time of the particles of the side. Thus the flow can be characterized as mixed.

8. Conclusion and Suggestions

In this research, the computational fluid dynamics technique was used to calibrate the parameters of the spring-dashpot model and compare their CFD-DEM simulation results of discharge time with the experimental results.

They were examined twenty-seven combinations of the parameters, coefficient of elasticity (K), coefficient of restitution (η), coefficient of static friction (μ_f) and coefficient of rolling friction (μ_r). The simulation results and statistical analysis indicated that the constant of elasticity (K) does not influence the model in question. The coefficient of restitution has negative effects, since when its value is high discharge time decreases. Since the coefficients of friction (μ_f) and rolling (μ_r) have a positive effect, so, its increase elevates the discharge times. It was identified that the variable that has the most significant is the coefficient of friction (μ_f).

The result closest to the experimental value was obtained in terms of coefficient of elasticity (K) of 400 N/m, coefficient of restitution (η) of 0.8; friction and rolling friction coefficients ($\mu_f = \mu_r = 0.25$) represent the best set of parameters among the analyzed, which correspond to simulation A1.

Through the best set of parameters and simulations, it was possible to characterize the flow stream as being mixed flow.

As suggestions for future work, it is possible to study different geometries of silos and hoppers, as well as different materials to analyze the different flow patterns that may exist in these equipments. It is also suggested the use of other numerical approaches, such as discrete element method (DEM) in specific software for this kind of simulation, to calibrate these types of equipment for soybean and other materials.

References

Almeida, N. P., Tavares, F. P., & Santos, K. G. (2015). Dinâmica das partículas de soja em tambor rotativo de bancada empregando elementos discretos. In *XXXVII Congresso Brasileiro de Sistemas Particulados, ENEMP 2015 [=Blucher Engineering Proceedings]. 2*, 47-65. São Paulo: Blucher. https://doi.org/10.5151/ENEMP2015-MS-404.

Araújo, B. S. A. (2014). *Fluidodinâmica Computacional dos Regimes de Escoamento do Leito de Jorro-Fluidizado com Tubo Draft.* [Trabalho de Conclusão de Curso, Universidade Federal do Triângulo Mineiro]. Uberaba, MG, Brasil.

Araújo, B. S. A., & Santos, K. G. (2017). CFD Simulation of Different Flow Regimes of the Spout Fluidized Bed with Draft Plates. *Materials Science Forum*, 899, 89-94.

Balevičius, R., Kačianauskas, R., Mrózc, Z., & Sielamowicz, I. (2011). Analysis and DEM simulation of granular material flow patterns in hopper models of different shapes. *Advanced Powder Technology*, 22(2), 226-235.

Batista, C. S. (2009). *Estudo teórico e experimental do fluxo de sólidos particulados em silos verticais.* [Doctoral Dissertation, Universidade Federal de Campina Grande]. Campina Grande, PB, Brasil. UFCG Repository.
http://dspace.sti.ufcg.edu.br:8080/jspui/bitstream/riufcg/1815/1/CL%C3%81UDIA%20DA%20SILVA%20BATISTA%20-%20TESE%20%28PPGEP%29%202009.pdf.

Batista Júnior, R., Vieira Neto, J. L., & Santos, K. G. (2019). Estudos de simulação CFD-DEM em um Leito de Jorro Cônico. *Revista Brasileira de Ciência, Tecnologia e Inovação*, 4, 284-294.

Béttega, R., Barrozo, M., Corrêa, R., & Freire, J. (2013). CFD simulation of heat transfer inside packed beds: Evaluation of effective thermal conductivity, *JP Journal of Heat and Mass Transfer*, 8(2), 137-148.

Bortolotti, C. T., Santos, K. G., Francisquetti, M. C. C., Duarte, C. R., & Barrozo, M. A. S. (2013). Hydrodynamic study of a mixture of west Indian cherry residue and soybean grains in a spouted bed. *The Canadian Journal of Chemical Engineering*, 91(11), 1871-1880.

Brown, C. J., & Nielsen, J. (1998). *Silos: fundamentals of theory, behaviour and design*. London: E & FN SPON. 836p.

Calil Junior, C., & Cheung, A. B. (2007). *Silos: pressões, fluxo, recomendações para o projeto e exemplos de cálculo*. ISBN: 978-85-85205-71-3. São Carlos: EESC-USP. 232p..

Cheung, A. B. (2007). *Modelo estocástico de pressões de produtos armazenados para a estimativa da confiabilidade estrutural de silos esbeltos*. [Doctoral Dissertation, Universidade de São Paulo]. São Carlos, SP, Brasil. Repository. https://teses.usp.br/teses/disponiveis/18/18134/tde-30102007-213438/publico/Tese_Andres_Batista_Cheung.pdf

Cundall, P. A., & Strack, O. D. L. (1979). A discrete numerical model for granular assemblies. *Geotechnique*, 29(1), 47-65.

Cunha, F. G., Santos, K. G., Ataíde, C. H., Epstein, N., & Barrozo, M. A. S. (2009). Annatto Powder Production in a Spouted Bed: An Experimental and CFD Study. *Industrial & Engineering Chemistry Research*, 48, 976-982.

Cunha, R. N., Santos, K. G., Lima, R. N., Duarte, C. R., & Barrozo, M. A. S. (2016). Repose angle of monoparticles and binary mixture: An experimental and simulation study. *Powder Technology*, 303, 203-211.

DIN 1055 (1987). *Design loads for buildings*: loads in silo bins. Berlin: Deutsche Norm. 6p.

Gravena, G. F., Vieira Neto, J. L., Santos, K. G., & Silvério, B. C. (2019). Estudo da influência dos coeficientes de atrito estático e fricção de rolamento em simulações DEM de tambores rotativos com suspensores. *Brazilian Journal of Development*, 5, 20800-20811.

Höhner, D. Wirtz, S., & Scherer, V. (2015). A study on the influence of particle shape on the mechanical interactions of granular media in a hopper using the Discrete Element Method. *Powder Technology*, 278, 286-305.

Jenike, A. W. (1964). *Storage and flow of silos*. Bulletin 123. Salt Lake City: University of Utah. 89p.

Justin, G. H. (2012). *Aplicação da fluidodinâmica computacional na avaliação da hidrodinâmica de estágio em colunas de destilação.* [Master's Thesis, Universidade Federal de São Carlos]. São Carlos, SP, Brasil. UFSCar Repository. https://repositorio.ufscar.br/handle/ufscar/4097?show=full.

Krawczyk, P., & Badyda, K. (2011). Two-dimensional CFD modeling of the heat and mass transfer process during sewage sludge drying in a solar dryer, *Archives of Thermodynamics*, 32, 3-16.

Lima, R. F. (2014). *Modelagem matemática do escoamento de grãos de soja em um secador com fluxo misto usando o método dos elementos discretos.* [Master's Thesis, Universidade Regional do Noroeste do Estado do Rio Grande do Sul]. Ijuí, RS, Brasil. UNIJUÍ Repository. http://bibliodigital.unijui.edu.br:8080/xmlui/bitstream/handle/123456789/2159/disserta%C3%A7%C3%A3o_rodolfo_lima_versao%20final.pdf?sequence=1.

Mantegazini, I. S., & Romero, O. J. (2019). Analysis of the flow in horizontal injector wells with profile equalization completion, *Research, Society and Development*, 8(9):e50891327.

Marques, I.I.D.R. (2013). *Investigação do Leito de Jorro como Reator em Potencial de Pirólise de Partículas Cartonadas*. [Master's Thesis, Universidade Federal de São Mateus]. São Mateus, ES, Brasil, UFES, Repository. http://portais4.ufes.br/posgrad/teses/tese_6749_Icaro%20Marques.pdf.

Medeiros, I. F. (2012). *Características de fluxo e vazão de descarga em silos verticais*. [Master's Thesis, Universidade Federal de Campina Grande]. Campina Grande, PB, Brasil. UFCG Repository. http://dspace.sti.ufcg.edu.br:8080/jspui/handle/riufcg/1078.

Müller, C. R., Scott, S. A., Holland, D. J., Clarke, B. C., Sederman, A. J., Dennis, J. S., & Gladden, L. F. (2009). Validation of a discrete element model using magnetic resonance measurements. *Particuology*, 7(4), 297-306.

Neto, J. L., Vieira, Martins, A. L., Neto, A., Silveira, Ataíde, C. H., & Barrozo, M. A. S. (2011). CFD applied to turbulent flows in concentric and eccentric annuli with inner shaft rotation. *The Canadian Journal of Chemical Engineering*. 89, 636-646.

Palma, G. (2005). *Pressões e Fluxo em Silos Esbeltos (h/d ≥ 1.5)*. [Master's Thesis, Universidade de São Paulo]. São Carlos, SP, Brasil. USP Repository. https://www.teses.usp.br/teses/disponiveis/18/18134/tde-09082005-141400/pt-br.php.

Pereira, A. S. et al. (2018). *Metodologia do trabalho científico*. [*e-Book*]. Santa Maria. Ed. UAB/NTE/UFSM. Available at: https://repositorio.ufsm.br/bitstream/handle/1/15824/Lic_Computacao_Metodologia-Pesquisa-Cientifica.pdf?sequence=1. Accessed on: April 4th, 2020.

Pereira, E. F. S., & Góis, L. M. N. (2020). Simulation of un industrial waste treatment tank, *Research, Society and Development*, 9(4), e180942542.

Rocha, A. A., Stoppe, A. C. R., Silvério, B. C., Santos, K. C., & Vieira Neto, J. L. (2020). Drying of malt residues in a solar greenhouse and in a fixed bed solar dryer. *Research, Society and Development*, 9(7):1-27, e447974335.

Santos, K. G., Ferreira, L. V., Santana, R. C., & Barrozo, M. A. S. (2017). CFD simulation of spouted bed working with a size distribution of sand particles: segregation aspects. *Materials Science Forum*, 899, 95-100.

Santos, K. G., Francisquetti, M. C. C., Malagoni, R. A., & Barrozo, M. A. S. (2015). Fluid Dynamic Behavior in a Spouted Bed with Binary Mixtures Differing in Size. *Drying Technology*, 33(14), 1746-1757.

Silvério, B. C., Santos, K. G., Duarte, C. R., & Barrozo, M. A. S. (2014). Effect of the Friction, Elastic, and Restitution Coefficients on the Fluid Dynamics Behavior of a Rotary

Dryer Operating with Fertilizer. *Industrial & Engineering Chemistry Research*, 53(21), 8920-8926.

Stoppe, A. C. R., Neto, J. L. V., & Santos, K. G. (2020). Development of a fixed bed solar dryer: experimental study and CFD simulation. *Research, Society and Development*, 9(3), e123932667.

Tegenaw, P. D., Gebrehiwot, M. G., & Vanierschot, M. (2019). On the comparison between computational fluid dynamics (CFD) and lumped capacitance modeling for the simulation of transient heat transfer in solar dryers. *Solar Energy,* 184, 417-425.

Vieira, L. H. S. (2009). *Estudo teórico e experimental de pressões em tremonhas cônicas e piramidais de silos metálicos esbeltos.* [Master's Thesis, Universidade Federal de Lavras]. Lavras, MG, Brasil. UFLA Repository.
http://repositorio.ufla.br/bitstream/1/3436/1/DISSERTA%C3%87%C3%83O_Estudo%20te%C3%B3rico%20e%20experimental%20das%20press%C3%B5es%20em%20tremonhas%20c%C3%B4nicas%20e%20piramidais%20de%20silos%20met%C3%A1licos%20esbeltos.pdf.

Vieira Neto, J. L., Duarte, C. R., Murata, V. V., & Barrozo, M. A. S. (2008). Effect of a Draft Tube on the Fluid Dynamics of a Spouted Bed: Experimental and CFD Studies. *Drying Technology*, 26(3), 299-307.

Vieira Neto, J. L., Martins, A. L., Ataíde, C. H., & Barrozo, M. A. S. (2014). The effect of the inner cylinder rotation on the fluid dynamics of non-Newtonian fluids in concentric and eccentric annuli. *Brazilian Journal of Chemical Engineering*, 31, 829-838.

Vieira Neto, J. L., Costa, D. D. L., Souza, L. V., Pires, R. F., Souza, D. L., Silvério, B. C., & Santos, K. G. (2017). A Fluid Dynamic Study in a Rotating Disk Applied in Granulation of Fertilizers. *Materials Science Forum,* 899, 142-147.
.

Research, Society and Development, v. 9, n. 8, e448985463, 2020
(CC BY 4.0) | ISSN 2525-3409 | DOI: http://dx.doi.org/10.33448/rsd-v9i8.5463

Percentage of contribution of each author in the manuscript

Jéssica Aparecida Apolinário de Paula – 50 %

Érica Victor de Faria – 10 %

Ana Christina Pitard Lima - 10 %

José Luiz Vieira Neto - 15 %

Kássia Graciele dos Santos - 15 %